Computers and Concrete, *Vol. 20, No. 1 (2017) 49-56*
DOI: https://doi.org/10.12989/cac.2017.20.1.049

Concrete compressive strength identification by impact-echo method

Chi-Che Hung[1a], Wei-Ting Lin[*2], An Cheng[2b] and Kuang-Chih Pai[1a]

[1]*Institute of Nuclear Energy Research, Atomic Energy Council, 1000 Wenhua Rd. Jiaan Village, Longtan District, Taoyuan City 32546, Taiwan*
[2]*Department of Civil Engineering, National ILan University, No.1, Sec. 1, Shennong Rd., Yilan City, Yilan County 26047, Taiwan*

(Received June 17, 2016, Revised March 20, 2017, Accepted March 21, 2017)

Abstract. A clear correlation exists between the compressive strength and elastic modulus of concrete. Unfortunately, determining the static elastic modulus requires destructive methods and determining the dynamic elastic modulus is greatly complicated by the shape and size of the specimens. This paper reports on a novel approach to the prediction of compressive strength in concrete cylinders using numerical calculations in conjunction with the impact-echo method. This non-destructive technique involves obtaining the speeds of P-waves and S-waves using correction factors through numerical calculation based on frequencies measured using the impact-echo method. This approach makes it possible to calculate the dynamic elastic modulus with relative ease, thereby enabling the prediction of compressive strength. Experiment results demonstrate the speed, convenience, and efficacy of the proposed method.

Keywords: compressive strength prediction; dynamic elastic modulus; P-wave speed; S-wave speed

1. Introduction

Non-destructive methods for the testing of concrete are crucial to identifying changes in the properties of concrete over time proposed by Sansalone (1997) and Carino (2013). Krauß (2006) and Voigt (2006) introduced ultrasonic testing methods by which to measure strength development in concrete during hardening. Wang (2012), Qixian (1996), and Hassan (2012) used this approach to investigate the effects of wave speed on the dynamic elastic modulus and Poisson's ratio of concrete. The impact-echo method is a type of ultrasonic testing used to assess the extent of cracking in concrete and locate interfaces between different materials. Hora *et al.* (2011) investigated the applicability of impulse-response and impact-echo acoustic methods in evaluating large-area concrete floors.

Poisson's ratio and elastic modulus are particularly important in assessing the physical and mechanical properties of materials. Standard design codes recommend estimating the elastic modulus of concrete based on the compressive strength values obtained on the 28th day. Shkolnik (2005), Gesoğlu (2002) and Panesar (2011) conducted extensive research on the link between elastic modulus and compressive strength. Demir (2005, 2008) estimated the elastic modulus from compressive strength using fuzzy logic and artificial neural networks, and compared their results with BS and ACI codes. The quality of concrete is generally estimated using in situ non-destructive testing methods, such as ultrasonic pulse velocity, wave reflection, ground penetrating radar, and the impact-echo method by Hoła (2010), Alani (2013), Saint-Pierre (2016) and Rehman (2016). Zhou (2015) indicated that using the relationship between structural design and field measurements to establish a good assessment model that includes the elastic modulus, strength, or other material parameters is crucial.

Researchers have adopted two approaches to the formulation of conversion models by which to assess compressive strength using measurements obtained via non-destructive methods. The first is the ordinary least squares method introduced by Ross (2009) and then modified by Mandel (1984) and Alwash (2016). The second is the calibration method using strength measurements obtained by coring, as proposed by Rojas-Henao (2012) and Pucinotti (2015). Unfortunately, this approach and requires verification using regression equations under various testing conditions. Researchers have demonstrated the use of impact-echo methods (using neural networks) to predict pull-off adhesion between layers of concrete. Sadowski (2016) proposed the use of impact-echo and impulse response methods (also using neural networks) for the identification of interlayer bonding in existing concrete. Garbacz (2015), Zhou (2016) and Gajzler (2016) observed that the aforementioned neural methods are often applied to locate de-bonding damage between concrete and rebar for repair works. Tayfur (2014), Yuan (2014), and Zhou (2016) also presented mathematical models to deal with this issue; however, further data collection is required to verify the efficacy of this approach.

The basic theory of ultrasonic wave propagation in a homogeneous, isotropic material was described by Malhotra (2003). The relationships among the parameters in an elastic solid are as follows

$$V_p = \sqrt{\frac{E_d(1-\upsilon)}{\rho(1+\upsilon)(1-2\upsilon)}} \quad (1)$$

∗Corresponding author, Assistant Professor
E-mail: wtlin@niu.edu.tw
[a]Ph.D.
[b]Professor

ISSN: 1598-8198 (Print), 1598-818X (Online)

$$V_s = \sqrt{\frac{E_d}{2\rho(1+\upsilon)}} \quad (2)$$

where, V_p and V_s respectively represent the velocities of compression waves (P-waves) and shear waves (S-waves); ρ is the density; υ is Poisson's ratio; and Ed is the dynamic modulus of elasticity. Combination of Eqs. (1) and (2) gives the following

$$\upsilon = \frac{2(\frac{V_s}{V_p})^2 - 1}{2(\frac{V_s}{V_p})^2 - 2} \quad (3)$$

$$E_d = {V_p}^2 \rho \frac{(1+\upsilon)(1-2\upsilon)}{(1-\upsilon)} \quad (4)$$

As long as ρ, V_p, and V_s are known, then the values of υ and Ed can be determined using Eqs. (3) and (4). As reported by Birgül (2009), it is possible to obtain V_p using sensors to measure the round trip of longitudinal waves transmitting through the material. Unfortunately, it is difficult to obtain V_s using the same approach, due to the rapid decrease in the energy of shear waves traveling through concrete.

Poisson's ratio is also difficult to obtain. Numerous researchers have demonstrated that Poisson's ratio can be derived as a definite value pertaining to the relationship between elastic modulus and compressive strength described by Han (2004) and Zhou (1995). Based on this relationship, we sought to formulate a simple, non-destructive method by which to obtain the longitudinal wave speed and shear wave speed. We hypothesize that this should make it possible to derive Poisson's ratio as well as the dynamic elastic modulus, thereby enabling accurate predictions of compressive strength.

2. Experimental

The objective of this study was to investigate the compressive strength of concrete using ASTM testing methods as well as the elastic modulus of concrete using the impact-echo method. Numerical predictions of compressive strength were compared with measurements obtained in experiments to verify the efficacy of this approach.

2.1 Concrete admixture

Type I Portland cement conforming to ASTM C150 was used in all experiments. Crushed calcareous stone (fineness modulus: 6.82; specific gravity: 2.73) was used as coarse aggregate. Quartz-based river sand (fineness modulus: 3.23; specific gravity: 2.70) was used as fine aggregate. Table 1 presents sieve analysis of the aggregate. It adopted three mix designs (Table 2) to examine the effects of curing age on the compressive strength and elasticity modulus of the resulting concrete. It also added superplasticizer to the admixture in accordance with ASTM C494 type G. All of the concrete specimens were mixed in our laboratory under strict quality control.

Table 1 Sieve analysis of fine and coarse aggregate

Sieve size (mm)	Passing (%)	
	Fine aggregate	Coarse aggregate
25.40	100	100
19.10	100	87.7
9.52	100	27.5
4.76	98.7	2.6
2.38	74.7	0
1.19	53.8	0
0.59	29.5	0
0.30	15.2	0
0.15	5.20	0

Table 2 Mixture design

	A	B	C
W/C	0.53	0.60	0.70
Water (kg/m^3)	194	215	244
Cement (kg/m^3)	370	361	351
Fine aggregate (kg/m^3)	795	775	754
Coarse aggregate (kg/m^3)	978	954	927
Admixture (kg/m^3)	1.85	1.81	1.76

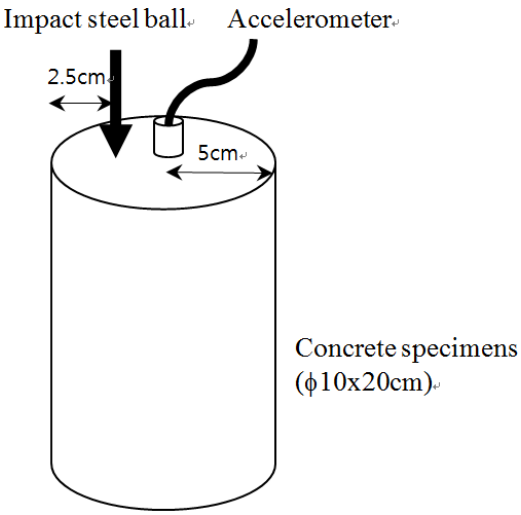

Fig. 1 Locations of impactor and accelerometer

2.2 Experiments

Cylindrical specimens (ϕ10×20 cm) made from each of the admixtures were tested at 28, 56, and 180 days to determine the elasticity modulus, wave speeds, and compressive strength. All measurements are presented as the average obtained from four specimens.

The static elastic modulus was measured in accordance with ASTM C469. We plotted the stress-strain curves obtained during testing, and the static modulus of elasticity was derived as follows

$$E_c = \frac{\sigma_2 - \sigma_1}{\varepsilon_2 - 0.00005} \quad (5)$$

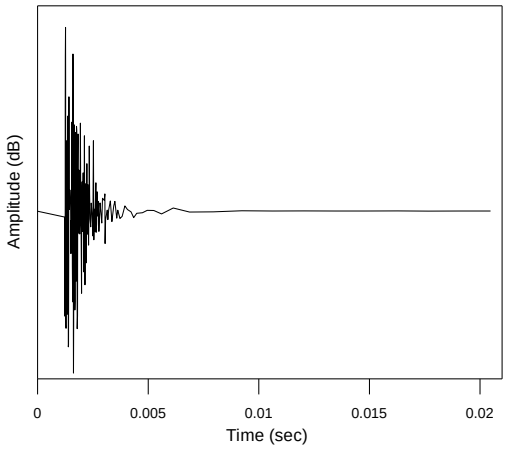

(a) Time-domain

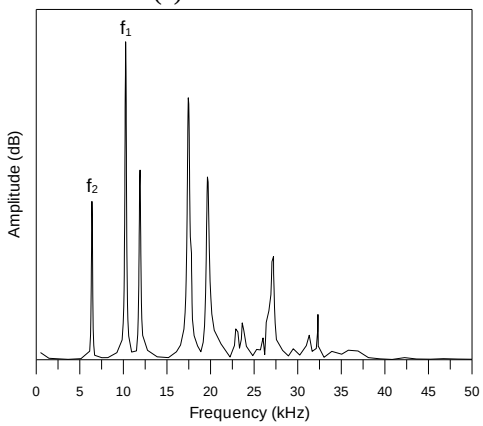

(b) Frequency-domain

Fig. 2 Diagrams showing response of concrete to impacts by steel ball

where E_c is the elastic modulus of elasticity, σ_2 is stress corresponding to 40% of ultimate load, σ_1=stress corresponding to a longitudinal strain of ε_{1at} 50 millionths (in psi), and ε_2 is longitudinal strain produced by stress σ_2.

The equipment used to measure wave speeds complies with Procedure B in ASTM C1383 (Impact-echo method). We employed a portable computer using a data-acquisition card with sampling rate>500 kHz. The impactor used in this experiment was a steel ball (diameter of 20 mm). The positions of the impactor and accelerometer are shown in Fig. 1. The response of the specimen to the impact with the steel ball was measured using an accelerometer. As shown in Fig. 2, this testing data was then used to obtain the natural (modal) frequency from the recorded waveform using the fast Fourier transform. The frequency was subsequently used to derive the speeds of P-waves and S-waves. As shown in Fig. 2(b), f_1 and f_2 represent the fundamental frequencies of the longitudinal (1st mode) and transverse vibration modes (2nd mode), respectively.

3. Results and discussion

3.1 Numerical calculations

Finite element analysis (FEM) was performed using ANSYS software, using brick elements (Solid65) for the three-dimensional modelling of cylindrical concrete specimens. Fig. 3 presents the 3D mesh used to model the concrete specimens. Eqs. (6) to (9) were used to derive the material properties of the concrete based on the speeds of S-waves and P-waves. It obtained the following results: elastic modulus (30 GPa), Poisson's ratio (0.2), and density (2300 kg/m^3). The transverse frequency (f_1) and longitudinal frequency (f_2) were obtained using modal analysis, as shown in Table 3.

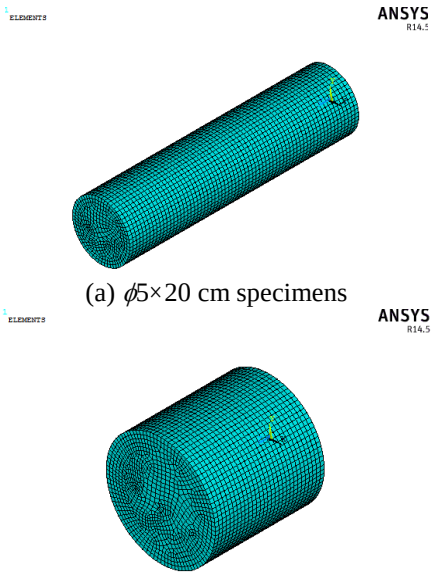

(a) ϕ5×20 cm specimens

(b) ϕ20×20 cm specimens

Fig. 3 FEM 3D mesh of specimens

In most practical applications, the speed of waves traveling through materials depends almost entirely on the material properties, rather than the size of the specimen. We can therefore surmise that for given material properties, the P and S wave speed can be calculated by multiplying the distance from double the length of the specimen by the frequency, as shown in Eqs. (6) and (7). In contrast, the natural (modal) frequency depends largely on the shape and/or size of materials through which the vibrations are passing. The relationship between the theoretical speed of the waves and the fundamental frequency of the vibrations was calculated using Eqs. (6) to (9). Eqs. (8) and (9) indicate as the parameters as the f_1/f_p and f_2/f_s.

$$V_p = 2Lf_p \tag{6}$$

$$V_s = 2Lf_s \tag{7}$$

$$\beta_p = \frac{f_1}{f_p} \tag{8}$$

$$\beta_s = \frac{f_2}{f_S} \tag{9}$$

where L is the length of the cylindrical specimen; f_p and f_s respectively represent the frequencies of longitudinal and shear waves taking a round trip along the long axis of the specimen. β_p and β_s respectively represent the correction factors for longitudinal and transverse vibrations. The

Table 3 Transverse and longitudinal frequencies in cylinders of various sizes

D/L	Calculated cylinder		Transverse frequency (Hz)	Longitudinal frequency (Hz)
	Diameter (cm)	Length (cm)		
0.167	5	30	1684	5858
0.167	10	60	849	2932
0.250	5	20	3549	8813
0.250	7.5	30	2365	5875
0.250	10	40	1770	4406
0.333	5	15	5855	11758
0.333	10	30	2923	5878
0.333	20	60	1462	2939
0.400	4	10	9868	17611
0.400	8	20	4934	8805
0.400	12	30	3288	5872
0.450	4.5	10	10541	17605
0.450	9	20	5271	8802
0.450	13.5	30	3511	5867
0.500	5	10	11140	17585
0.500	10	20	5577	8794
0.500	15	30	3706	5862
0.500	20	40	2780	4397
0.550	5.5	10	11690	17568
0.550	11	20	5869	8784
0.550	16.5	30	3906	5856
0.600	6	10	12217	17542
0.600	12	20	6104	8771
0.600	18	30	4069	5847
0.667	10	15	8553	11668
0.667	20	30	4265	5831
0.667	40	60	2133	2916
0.750	15	20	6746	8718
0.750	30	40	3373	4359
1.000	10	10	14790	17050
1.000	20	20	7388	8525
1.000	40	40	3698	4263

correction factor is the ratio of the modal frequency to the frequency of the waves. β_p and β_s are the ratios of the frequencies of the 1st and 2nd modes divided by the frequencies of the P and S waves, respectively.

Fig. 4 illustrates the relationship between the diameter-length ratio and the correction factor. The regression equations are presented as Eqs. (10) and (11), where the R^2 of β_p is 0.996 and the R^2 of β_s is 0.997. The ratio of modal frequency to wave frequency is nearly the same as the ratio of diameter to length, regardless of the overall size of the specimen. It was found that the ratio of the diameter to length was an important variable. The ratio of diameter to length was between 0.167 and 1; therefore, the correction factors are as follows: longitudinal waves (0.915-0.947) and shear waves (0.443-1.296). The size of the cylindrical

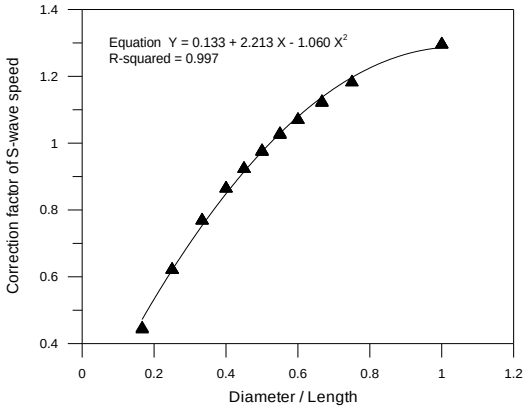

(a) S-wave speed

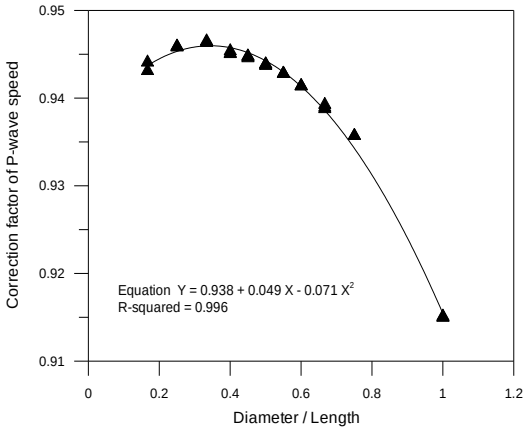

(b) P-wave speed

Fig. 4 Relationship between correction factor and diameter/length ratio

specimens was shown to greatly influence the speed of shear waves.

$$\beta_s = 0.133 + 2.213\frac{D}{L} - 1.060\left(\frac{D}{L}\right)^2 \quad (10)$$

$$\beta_p = 0.938 + 0.049\frac{D}{L} - 0.071\left(\frac{D}{L}\right)^2 \quad (11)$$

3.2 Density, strength and static elastic modulus

Table 4 lists the results of experiments aimed at determining the density, compressive strength, and static elastic modulus of the concrete specimens. Four specimens from each of the three admixtures (groups A, B, and C from Table 2) were subjected to all three of the tests at 28, 56, and 180 days. In the first column of Table 4, the letters A, B, and C indicate the three different w/c ratios in Table 2. A1-A3 represents 3 specimens of the same age. The measurement results are presented as the average of the four specimens in each group. The coefficient of variation was controlled to less than 5%. The water-cement ratio of group A was lower than that of groups B and C, which produced greater compactness. As a result, the density, compressive strength and static elastic modulus of specimens in group A were higher than those in groups B and C. The elastic modulus has a greater effect on compressive strength than

Table 4 Density, compressive strength, and static elastic modulus of concrete specimens

Mix No.	Density (kg/m^3)	Compressive strength (MPa)			Static modulus of elasticity (GPa)		
		Day 28	Day 56	Day 180	Day 28	Day 56	Day 180
A1	2442	34.1	44.7	38.6	17.6	24.1	27.1
A2	2434	29.0	32.7	45.7	15.3	24.5	28.7
A3	2448	39.3	48.5	49.3	17.5	24.9	27.9
A4	2482	37.3	47.8	57.7	18.1	28.0	28.6
B1	2430	26.0	43.0	47.7	14.5	24.6	27.6
B2	2419	25.9	44.3	46.6	14.8	25.1	26.8
B3	2388	29.6	40.1	45.1	15.0	23.1	26.8
B4	2407	28.6	41.7	47.7	15.7	23.8	26.0
C1	2347	16.9	27.4	29.9	11.7	19.0	21.7
C2	2342	16.9	24.9	30.4	13.7	19.1	21.1
C3	2334	23.6	27.8	27.0	14.8	19.2	22.1
C4	2318	15.8	20.5	29.5	13.4	16.4	22.4

Table 5 Wave speed and Poisson's ratio of concrete specimens

Mix No.	S-wave speed (m/s)			P-wave speed (m/s)			Poisson's ratio		
	Day 28	Day 56	Day 180	Day 28	Day 56	Day 180	Day 28	Day 56	Day 180
A1	2269	2544	2646	3843	4279	4444	0.233	0.227	0.225
A2	2277	2503	2663	3886	4279	4415	0.239	0.240	0.214
A3	2306	2544	2658	3843	4258	4415	0.219	0.223	0.216
A4	2265	2544	2663	3776	4258	4423	0.219	0.223	0.216
B1	2162	2466	2572	3657	4182	4301	0.231	0.234	0.221
B2	2224	2498	2564	3699	4246	4258	0.217	0.235	0.216
B3	2244	2466	2605	3708	4250	4339	0.211	0.246	0.218
B4	2285	2523	2544	3780	4229	4258	0.212	0.224	0.223
C1	2014	2322	2445	3369	3886	4042	0.222	0.222	0.212
C2	2170	2343	2404	3543	3907	4030	0.200	0.219	0.224
C3	2162	2338	2404	3598	3949	4008	0.217	0.230	0.219
C4	2183	2343	2425	3611	3949	4059	0.212	0.229	0.223

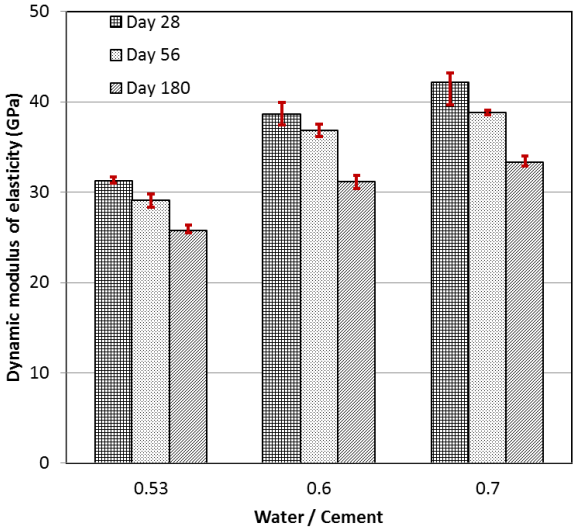

Fig. 5 Dynamic elastic modulus in specimens with various water/cement ratio

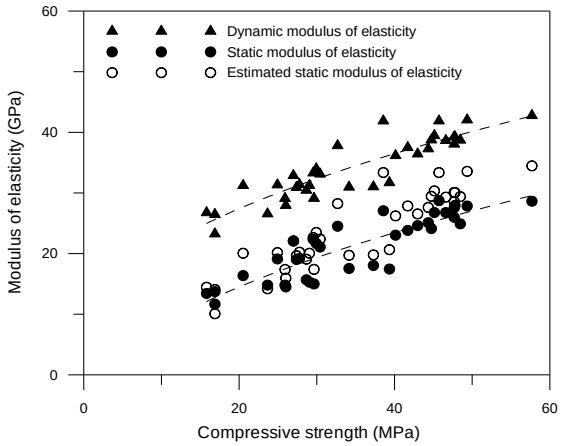

Fig. 6 Relationship between elastic modulus and compressive strength

does density. In fact, no obvious relation exists between Poisson's ratio and compressive strength. Thus, efforts to predict the compressive strength of concrete are generally based solely on the modulus of elasticity.

3.3 Wave speeds

Table 5 lists the speeds of S-waves and P-waves obtained using the impact-echo method. The frequencies of the longitudinal and transverse vibrations were derived from the resonance of the specimens. The speeds of S-waves and P-waves were calculated using Eqs. (12) and (13) with correction factors, where β_p=0.945 and β_s=0.975 and D/L=0.5 is a constant. Deriving the speed of S-waves in concrete is normally very difficult; however, the proposed impact-echo method makes it possible to produce S-waves without the need for expensive ultrasonic instruments.

$$V_p = \frac{2Lf_1}{\beta_p} \tag{12}$$

$$V_s = \frac{2Lf_2}{\beta_s} \tag{13}$$

The ratio of S-wave speed to P-wave speed was 0.59-0.61. From the speeds of S-waves and P-waves, we derived a Poisson's ratio of 0.21-0.23; however, this value did not appear to vary with curing age or water-cement ratio. As shown in Fig. 5, we also derived the dynamic elastic modulus of concrete from the speeds of S-waves and P-waves using Eq. (4). This value was shown to vary with curing age and the design of the admixture. For example, the dynamic elastic modulus was shown to increase with an increase in compressive strength, a reduction in the water-cement ratio, or an increase in curing age.

3.4 Relationship between elastic modulus and strength

As shown in Fig. 6, the dynamic and static elastic moduli are both functions of compressive strength. Furthermore, the static elastic modulus is correlated with the dynamic elastic modulus; i.e., it can be calculated from

the dynamic elastic modulus using Eq. (14), proposed by British Standards (1972). As shown in Fig. 6, the predictions for static elastic modulus are close to the values obtained in testing.

$$E_c = 1.25E_d - 19 \quad (14)$$

The regression relationship between the elastic modulus and compressive strength in Fig. 6 can be obtained using Eqs. (15) and (16); their correlation coefficients R^2 are 0.67 and 0.80, respectively. These results indicate that the correlation between dynamic elastic modulus and compressive strength is stronger than that between static elastic modulus and compressive strength. In other words, predictions of compressive strength based on the dynamic elastic modulus are more reliable than those based on the static elastic modulus.

$$E_c = 4.83\sqrt{\sigma} - 7.10 \quad (15)$$

$$E_d = 4.90\sqrt{\sigma} + 5.5 \quad (16)$$

Fig. 7 presents a comparison of compressive strength predictions obtained using various equations. The predictions obtained using Eq. (16) are superior to those obtained using Eq. (17) (ACI 318 1995), Eq. (18) (ACI 363 1984), Eq. (19) (BS 1972), and Eq. (20) (Hansen 1986).

$$E_c = 0.0000427\rho^{1.5}\sqrt{\sigma} \quad (17)$$

$$E_c = \left(3.321\sqrt{\sigma} + 6.895\right)\left(\frac{\rho}{2300}\right)^{1.5} \quad (18)$$

$$E_d = 2.8\sqrt{\sigma} + 22 \quad (19)$$

$$E_d = 5.31\sqrt{\sigma} + 5.83 \quad (20)$$

Fig. 7(a) presents the compressive strength results obtained after curing for 28 days. Despite the fact that the values for static elastic modulus and dynamic elastic modulus were obtained using different methods, all of the predicted values are lower than those obtained in experiments; i.e., all of the predicted values fell below the dotted line in the figure. Regardless of the standards employed, all of the predictions pertaining to compressive strength were conservative.

As shown in Figs. 7(b) and 7(c), our predictions of compressive strength at 56 and 180 days (based on dynamic elastic modulus) are closely correlated with the values obtained in experiments. From this we can infer that the dynamic elastic modulus is more strongly associated with compressive strength than is the static elastic modulus. The regression coefficients in Eqs. (15) and (16) (R^2: 0.80>0.67) indicate a better regression relationship between Ed and compressive strength. These findings demonstrate the feasibility of formulating predictions of compressive strength from the dynamic elastic modulus. The implementation of the proposed non-destructive method would make it possible to perform strength tests repeatedly on a single cylindrical specimen, thereby greatly reducing the number of specimens that are routinely lost to destructive testing in the continual monitoring of changes in concrete strength over time.

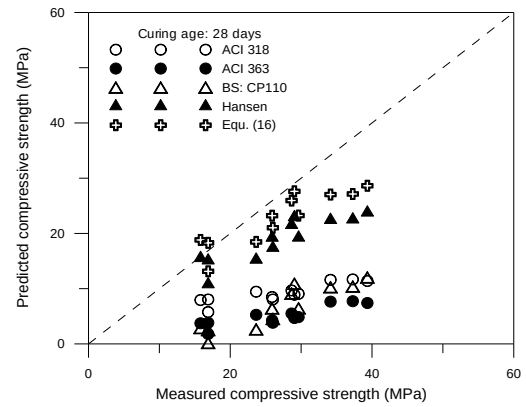

(a) 28 days

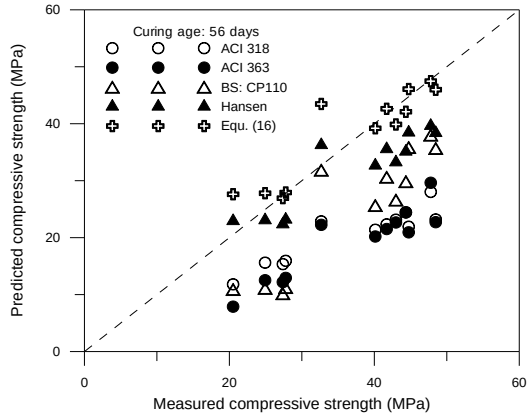

(b) 56 days

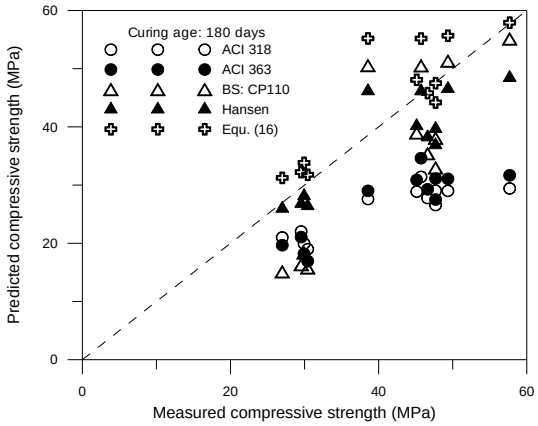

(c) 180 days

Fig. 7 Correlation between predicted values and measured values for compressive strength

4. Conclusions

This paper reports a rapid, non-destructive approach to predicting the compressive strength of concrete cylinders based on the dynamic elastic modulus. We propose the use of a correction factor to facilitate calculating the speeds of S-waves and P-waves from the frequencies of transverse and longitudinal vibration modes. From these speeds it is possible to determine the dynamic elastic modulus, which is closely correlated with compressive strength. Our experiment results indicate that the link between dynamic elastic modulus and compressive strength is stronger than that between the static elastic modulus and compressive

strength. These findings demonstrate the feasibility of formulating predictions of compressive strength from the dynamic elastic modulus.

References

ACI Committee 318 (1996), *Building Code Requirements for Structural Concrete, ACI Manual of Concrete Practice Part 3: Use of Concrete in Buildings-Design, Specifications, and Related Topics*, Detroit, Michigan, U.S.A.

ACI Committee 363 (1984), "State-of-art-report on high strength concrete", *ACI Mater. J.*, **81**(4), 364-411.

Alani, A.M., Aboutalebi, M. and Kilic, G. (2013), "Applications of ground penetrating radar (GPR) in bridge deck monitoring and assessment", *J. Appl. Geophys.*, **97**, 45-54.

Alwash, M., Sbartaï, Z.M. and Breysse, D. (2016), "Non-destructive assessment of both mean strength and variability of concrete: A new bi-objective approach", *Constr. Build. Mater.*, **113**, 880-889.

Birgül, R. (2009), "Hilbert transformation of waveforms to determine shear wave velocity in concrete", *Cement Concrete Res.*, **39**(8), 696-700.

British Standards Institution (1972), *The Structural Use of Concrete. Part 1: Design, Materials and Workmanship*, London, U.K.

Carino, N.J. (2013), "Training: Often the missing link in using NDT methods", *Constr. Build. Mater.*, **38**, 1316-1329.

Demir, F. (2005), "A new way of prediction elastic modulus of normal and high strength concrete-fuzzy logic", *Cement Concrete Res.*, **35**(8), 1531-1538.

Demir, F. (2008), "Prediction of elastic modulus of normal and high strength concrete by artificial neural networks", *Constr. Build. Mater.*, **22**(7), 1428-1435.

Demir, F. and Korkmaz, K.A. (2008), "Prediction of lower and upper bounds of elastic modulus of high strength concrete", *Constr. Build. Mater.*, **22**(7), 1385-1393.

Gajzler, M. (2016), "Supporting of repairs processes of concrete industrial floors", *Eng. Struct. Technol.*, **8**(1), 8-14.

Garbacz, A. (2015), "Application of stress based NDT methods for concrete repair bond quality control", *Bull. Pol. Acad. Sci. Technol. Sci.*, **63**(1), 77-85.

Gesoğlu, M., Güneyisi, E. and Özturan, T. (2002), "Effects of end conditions on compressive strength and static elastic modulus of very high strength concrete", *Cement Concrete Res.*, **32**(10), 1545-1550.

Han, S.H. and Kim, J.K. (2004), "Effect of temperature and age on the relationship between dynamic and static elastic modulus of concrete", *Cement Concrte Res.*, **34**(7), 1219-1227.

Hansen, T.C. (1986), "Recycled aggregate and recycled aggregate concrete", *Mater. Struct.*, **19**(3), 201-204.

Hassan, A.M.T. and Jones, S.W. (2012), "Non-destructive testing of ultra high performance fibre reinforced concrete (UHPFRC): A feasibility study for using ultrasonic and resonant frequency testing techniques", *Constr. Build. Mater.*, **35**, 361-367.

Hoła, J. and Schabowicz, K. (2010), "State-of-the-art non-destructive methods for diagnostic testing of building structures-anticipated development trends", *Arch. Civil Mech. Eng.*, **10**(3), 5-18.

Hoła, J., Sadowski, L. and Schabowicz, K. (2011), "Nondestructive identification of delaminations in concrete floor toppings with acoustic methods", *Automat. Constr.*, **20**(7), 799-807.

Krauß, M. and Hariri, K. (2006), "Determination of initial degree of hydration for improvement of early-age properties of concrete using ultrasonic wave propagation", *Cement Concrete Compos.*, **28**(4), 299-306.

Malhotra, V.M. and Carino, N.J. (2003), *Handbook on Nondestructive Testing of Concrete*, CRC Press, New York, U.S.A.

Panesar, D.K. and Shindman, B. (2011), "Elastic properties of self-consolidating concrete", *Constr. Build. Mater.*, **25**(8), 3334-3344.

Pucinotti, R. (2015), "Reinforced concrete structure: Nondestructive in situ strength assessment of concrete", *Constrs Build. Mater.*, **75**, 331-341.

Qixian, L. and Bungey, J.H. (1996), "Using compression wave ultrasonic transducers to measure the velocity of surface waves and hence determine dynamic modulus of elasticity for concrete", *Constr. Build. Mater.*, **10**(4), 237-242.

Rehman, S.K.U., Ibrahim, Z., Memon, S.A. and Jameel, M. (2016), "Nondestructive test methods for concrete bridges: A review", *Constr. Build. Mater.*, **107**, 58-86.

Rojas-Henao, L., Fernández-Gómez, J. and López-Agüí, J. (2012), "Rebound hammer, pulse velocity and core tests in self-consolidating concrete", *ACI Mater. J.*, **109**(2), 235-243.

Ross, M.S. (2009), *Introduction to Probability and Statistics for Engineers and Scientists*, 4th Edition, Elsevier Inc., U.S.A.

Sadowski, Ł., Hoła, J. and Czarnecki, S. (2016), "Non-destructive neural identification of the bond between concrete layers in existing elements", *Constr. Build. Mater.*, **127**, 49-58.

Saint-Pierre, F., Philibert, A., Giroux, B. and Rivard, P. (2016), "Concrete quality designation based on ultrasonic pulse velocity", *Constr. Build. Mater.*, **125**, 1022-1027.

Sansalone, M. (1997), "Impact-echo: The complete story", *ACI Struct. J.*, **94**(6), 777-786.

Shkolnik, I.E. (2005), "Effect of nonlinear response of concrete on its elastic modulus and strength", *Cement Concrete Compos.*, **27**(7-8), 747-757.

Tayfur, G., Erdem, T.K. and Kirca, Ö. (2014), "Strength prediction of high-strength concrete by fuzzy logic and artificial neural networks", *J. Mater. Civil Eng.*, **26**(11), 040140791-040140797.

Voigt, T., Sun, Z. and Shah, S.P. (2006), "Comparison of ultrasonic wave reflection method and maturity method in evaluating early-age compressive strength of mortar", *Cement Concrete Compos.*, **28**(4), 307-316.

Wang, J.J., Chang, T.P., Chen, B.T. and Wang, H. (2012), "Determination of Poisson's ratio of solid circular rods by impact-echo method", *J. Sound Vibr.*, **331**(5), 1059-1067.

Yıldırım, H. and Sengul, O. (2011), "Modulus of elasticity of substandard and normal concretes", *Constr. Build. Mater.*, **25**(4), 1645-1652.

Yuan, Z., Wang, L.N. and Ji, X. (2014), "Prediction of concrete compressive strength: Research on hybrid models genetic based algorithms and ANFIS", *Adv. Eng. Softw.*, **67**, 156-163.

Zhou, F.P., Lydon, F.D. and Barr, B.I.G. (1995), "Effect of coarse aggregate on elastic modulus and compressive strength of high performance concrete", *Cement Concrete Res.*, **25**(1), 177-186.

Zhou, J., Ye, G. and Breugel, K. (2016), "Cement hydration and microstructure in concrete repairs with cementitious repair materials", *Constr. Build. Mater.*, **112**, 765-772.

Zhou, Q., Wang, F. and Zhu, F. (2016), "Estimation of compressive strength of hollow concrete masonry prisms using artificial neural networks and adaptive neuro-fuzzy inference systems", *Constr. Build. Mater.*, **127**, 417-426.

Zhou, Y., Gao, J., Sun, Z. and Qu, W. (2015), "A fundamental study on compressive strength, static and dynamic elastic moduli of young concrete", *Constr. Build. Mater.*, **98**, 137-145.

CC

APPENDIX: Index of special acronyms

V_p	Velocities of compression wave (P-wave)
V_s	Velocities of shear wave (S-wave)
E_d	Dynamic modulus of elasticity
ρ	Density
ν	Poisson's ratio
W/C	Water/cement ratio
E_c	Elastic modulus of elasticity
σ_1	Stress corresponding to a longitudinal strain of 50 millionths
σ_2	Stress corresponding to 40 % of ultimate load
ε_2	Longitudinal strain produced by stress σ_2
L	Length of the cylinder specimen
D	Diameter of the cylinder specimen
f_p:	Longitudinal wave frequency of a round trip along the axis of the cylinder specimen
f_s:	Shear wave frequency of a round trip along the axis of the cylinder specimen
β_p	Correction factor on the longitudinal vibration mode
β_s	Correction factor on the transverse vibration mode
f_1	Fundamental frequency on the longitudinal vibration mode
f_2	Fundamental frequency on the transverse vibration mode
σ	Predicted compressive strength